CAPACITY IMPROVEMENT OF CELLULAR CDMA BY THE SUBSPACE-TRACKING ARRAY-RECEIVER

Sofiène AFFES and Paul MERMELSTEIN

INRS-Télécommunications, Université du Québec
16, Place du Commerce, Ile des Soeurs, Verdun, QC, H3E 1H6, Canada
Tel: (1) (514) 765.7817/7349 - Fax: (1) (514) 761.8501
E-mail: affes@inrs-telecom.uquebec.ca

ABSTRACT

Based on a new formulation derived from array signal processing theory, we develop in this contribution the Subspace-Tracking Array-Receiver (STAR) for cellular CDMA in a multipath environment. The new receiver, STAR, shows fast tracking capability in the presence of strong nonstationarities, requires a low order of computational complexity and increases the uplink capacity of the CDMA system in terms of number of users per cell.

1. NEW FORMULATION AND MODELING

The application of array signal processing techniques to wireless communications is of significant current research interest. These techniques are very promising particularly in cellular CDMA [1], after Suard *et al.* [2] and Naguib and Paulraj [3], and others, first introduced array beamforming in a 2D-RAKE receiver. Here, we propose a Subspace-Tracking Array-Receiver, STAR. This new receiver has a very simple structure and outperforms [2] and [3] in capacity by almost a factor of 2.

We consider a CDMA cellular system with base-stations equipped with a receiving antenna of M sensors. We assume that U is the number of users received by this antenna. The PSK bit sequence of each user is first differentially encoded (*i.e.* DPSK) at the rate $1/T$ where T is the bit duration. Then it is spread by a personal code at the rate $1/T_c$ with a processing gain defined by $L = T/T_c$, where T_c is the chip pulse duration. We also assume a multipath environment, where P is the number of paths.

At time t, the observation vector received by the antenna array can be written as follows:

$$X(t) = \sum_{i=1}^{U}\sum_{p=1}^{P} X_{i,p}(t) + \mathcal{N}(t) , \qquad (1)$$

where:

$$X_{i,p}(t) = \frac{\rho_i(t)}{r_i^d(t)}\mathcal{G}_{i,p}(t)a_i(t-\tau_{i,p}(t))b_i(t-\tau_{i,p}(t))c_i(t-\tau_{i,p}(t)).$$

In (1), $b_i(t)$ is a DPSK sequence of the i^{th} user and $a_i^2(t)$ is its controlled power at transmission. For the sake of simplicity and without loss of generality, the spreading code $c_i(t)$ of the i^{th} user is assumed to be periodical with period T. Over each bit duration $t \in [0, T[$, the code period is obtained by a personal random binary PN sequence of length L spread by a given chip pulse with any time-limited shape over $[0, T_c[$. The M-dimensional complex vector $\mathcal{G}_{i,p}(t)$ and $\tau_{i,p}(t) \in [0, T[$ respectively denote the fading and the array response from the i^{th} user to the antenna elements of the base-station and the propagation time delay along the p^{th} path. We assume here both multipath channel parameters to be slowly varying in time and locally constant as compared to the bit duration T. The effects of the shadowing and the path loss are respectively modeled by $\rho_i(t)$ and $r_i^d(t)$ where $r_i(t)$ is the distance from the user to the base-station and d is the path loss exponent. We assume their variations in time to be very slow as compared to T, so that they are nearly constant over several bit durations. For power control, $a_i(t)$ is updated at the bit rate $1/T$ so that $a_i(t - \tau_{i,p}(t)) \simeq a_i(t)$. Finally, the M-dimensional complex vector $\mathcal{N}(t)$ denotes the additive thermal noise received at the antenna elements.

Without loss of generality, we consider that the index, say $i_0 \in \{1, \cdots, U\}$, refers to the user of interest located in the cell covered by the base-station. For the sake of simplicity, we actually omit the index i_0 and reformulate Eq. (1) as:

$$X(t) = \psi(t)\sum_{p=1}^{P} G_p(t)\varepsilon_p(t)b(t - \tau_p(t))c(t - \tau_p(t)) + \mathcal{I}(t) , \qquad (2)$$

where $\mathcal{I}(t)$ denotes the noise term due to thermal noise and to the interference from the other users. Along the p^{th} path, $G_p(t) = \left(\sqrt{M}/\,\|\mathcal{G}_{i_0,p}(t)\|\right)\mathcal{G}_{i_0,p}(t)$ is a propagation vector with norm $\sqrt{M}$ and $\varepsilon_p^2(t) = \|\mathcal{G}_{i_0,p}(t)\|^2 / \sum_{k=1}^{P}\|\mathcal{G}_{i_0,k}(t)\|^2$ is the fraction of the total power

$$\psi^2(t) = \left(\rho_{i_0}(t)/r_{i_0}^d(t)\right)^2 a_{i_0}^2(t)\sum_{p=1}^{P}\|\mathcal{G}_{i_0,p}(t)\|^2 / M$$

received from the desired user (*i.e.* $\sum_{p=1}^{P}\varepsilon_p^2(t) = 1$). In this new equation, we normalized all the quantities involved in the classical model of Eq. (1) and confined their power variations in the total received power $\psi^2(t)$. This simple reformulation is more appropriate to array signal processing techniques.

2. THE PROPOSED STRUCTURE OF STAR

We assume that the multipath time delays $\tau_p(t)$ are perfectly estimated and tracked as in [2],[3]. Since the time-delay synchronization and tracking (see [1]) are not the focus of this paper, we assume the multipath delays to be constant in time (*i.e.* $\tau_p(t) = \tau_p$). The variable-delay problem will actually be addressed in a future publication as a generalization of this work [4].

At this stage we define at the p^{th} path the post-correlated observation vector at the discrete time indexes $n = 0, 1, 2, \cdots$ by:

$$Z_{p,n} = \frac{1}{T}\int_0^T X(t + \tau_p + nT)c(t)dt\ , \qquad (3)$$

and have:

$$Z_{p,n} = \psi_n G_{p,n}\varepsilon_{p,n}b_n + N_{p,n} = G_{p,n}s_{p,n} + N_{p,n}\ . \qquad (4)$$

By virtue of the stationarity assumptions stated earlier, we assumed in the development of Eq. (4) that $\psi(t+\tau_p+nT)$, $G_p(t + \tau_p + nT)$ and $\varepsilon_p(t + \tau_p + nT)$ are constant during the integration interval $t \in [0, T]$ and respectively equal to ψ_n, $G_{k,n}$ and $\varepsilon_{k,n}$ for $k, p \in \{1, \cdots, P\}$. On the other hand, the sequence $b(t + nT)$ is constant over the bit duration T and equal to b_n for $t \in [0, T]$, while $c(t + nT)$ is periodical of period T and equal to $c(t)$.

In Eq. (4), we have for each path a classical equation of a narrowband instantaneous mixture model where $s_{p,n}$ is the signal component. At this point, we can apply array signal processing techniques developed in [5],[6] for subspace-tracking to adaptively identify $G_{p,n}$ and extract $s_{p,n}$.

We next explain the structure of STAR. Assume that estimates of $G_{p,n}$ say $\hat{G}_{p,n}$ are available at each iteration n. We explain below how to track $G_{p,n}$ by a subspace-based tracking procedure. From these estimates, we can extract the signal component $s_{p,n}$ for $p \in \{1, \cdots, P\}$ by any distortionless beamformer $W_{p,n}$ (*i.e.* $W^H_{p,n}\hat{G}_{p,n} = 1$). For the sake of simplicity (see discussion in section 3), $N_{p,n}$ can be reasonably approximated as uncorrelated white noise for which a Delay-Sum (DS) beamformer (*i.e.* $W_{p,n} = \hat{G}_{p,n}/M$) is optimal for source extraction:

$$\hat{s}_{p,n} = \text{Real}\left\{W^H_{p,n}Z_{p,n}\right\} = \text{Real}\left\{\frac{\hat{G}^H_{p,n}Z_{p,n}}{M}\right\}\ . \qquad (5)$$

Note that the Real{.} function in (5) extracts the real sequence $s_{p,n} = \psi_n\varepsilon_{p,n}b_n$ and further reduces the power of the residual interference in $\hat{s}_{p,n}$ by half, contrary to [2],[3]. Actually, instead of the DS beamformer, a Generalized Sidelobe Canceler (GSC) structure can be selected to adaptively implement the Linearly Constrained Minimum Variance (LCMV) beamformer [6]. This beamformer, whose incorporation is presently under study, is shown [6] to be optimal for coherent source extraction in colored noise under some linear constraints such as null constraints.

Next we address the problem of power estimation and control. The total power received from the desired user can be estimated as follows:

$$\hat{\psi}^2_n = (1-\alpha)\ \hat{\psi}^2_{n-1} + \alpha\sum_{p=1}^{P}|\hat{s}_{p,n}|^2\ , \qquad (6)$$

where $\alpha \ll 1$ is a smoothing factor of the power estimate. To obtain Eq. (6), we have used $\sum_{p=1}^{P}\hat{\varepsilon}^2_{p,n} = 1$. For power control, ψ^2_n should be confined to the desired total received power say ψ^2_{opt} within an acceptable relative deviation, say $\delta_\psi \ll 1$. The control is achieved over the transmitted power $a^2(t)$ in (1) using the following rule:

$$a^2_{n+1} = \begin{cases} (1-\delta_a)\ a^2_n & \text{if}\ \ \hat{\psi}^2_n > (1+\delta_\psi)\ \psi^2_{\text{opt}}\ , \\ (1+\delta_a)\ a^2_n & \text{if}\ \ \hat{\psi}^2_n < (1-\delta_\psi)\ \psi^2_{\text{opt}}\ , \\ a^2_n & \text{otherwise.} \end{cases} \qquad (7)$$

The increment $\delta_a \ll 1$ is the relative change in power transmitted by the user. Notice here that a one-threshold rule can be easily used instead of (7). Although the power control is formulated for an adaptation at each bit duration T, in practice the changes can be made less frequently at larger time intervals.

Now the DPSK bit sequence b_n can be directly estimated by the following decision equation:

$$\hat{b}_n = \text{Sign}\left\{\tilde{b}_n\right\}\ , \qquad \tilde{b}_n = \sum_{p=1}^{P}\frac{|\hat{s}_{p,n}|}{\hat{\psi}^2_n}\hat{s}_{p,n}\ , \qquad (8)$$

where $\tilde{b}_n$ is the decision variable. Note that this equation can be easily adapted to other constellations. Contrary to [2],[3], we apply in (8) optimum gain combining instead of equal gain combining. In addition, we only use the beamformer outputs at the current sampling instants instead of the current and previous sampling instants. In [3], the source components $s_{p,n}$ are estimated over the P paths within unknown phase shifts. Hence the previous samples are required to compensate the phase shifts in the decision variable of [3]. On the other hand, we take advantage of the constant modulus property in Eq. (8) and reduce these phase shifts to a simple sign ambiguity as shown below.

Indeed, we separately track each propagation vector $G_{p,n}$ for $p = 1, \cdots, P$, by the following subspace-based tracking procedure [5],[6]:

$$\hat{G}_{p,n+1} = \hat{G}_{p,n} + \mu_{p,n}(Z_{p,n} - \hat{G}_{p,n}\hat{s}_{p,n})\hat{s}^*_{p,n}\ , \qquad (9)$$

where $\mu_{p,n}$ is an adaptation step-size, possibly normalized, and $*$ denotes complex conjugation.

A similar equation was first proposed in [7] for principal component analysis in neural networks. As shown in [8], this equation adaptively converges in the general case to the eigenvector associated with the largest eigenvalue of R_{Z_p}, where $R_{Z_p} = E[Z_{p,n}Z^H_{p,n}]$ is the post-correlation covariance matrix over the p^{th} path. Assuming the noise $N_{p,n}$ in (4) to be white and uncorrelated as stated earlier, Eq. (9) converges to $G_{p,n}$ for $p = 1, \cdots, P$, within unknown phase shifts. In this case, the source components $s_{p,n}$ manifest the opposite phase shifts in (5). However, using the Real{.} function in (5) forces back these phase shifts to adapt all to either 0 or π.

This constant modulus property of the DPSK sequence b_n, implemented in (9) through $\hat{s}_{p,n}$, finally guarantees convergence within a sign ambiguity (*i.e.* $\hat{G}_{p,n} \simeq \pm G_{p,n}$ when $n \to \infty$). This ambiguity has no consequences other than changing the signs of $\hat{s}_{p,n}$ and $\hat{b}_n$ in (5) and (8) respectively, since b_n is a DPSK sequence.

3. PERFORMANCE EVALUATION

We compare in this section the performance of the proposed algorithm with the techniques developed in [2],[3]. In these contributions, the spatially colored noise case is advantageously addressed. Usually, with a uniform distribution of users, the noise is colored when the number of users in the system is small. Under this condition, their total interference is relatively small and significantly reduced after correlation and has a negligible effect on the structure of the post-correlation covariance matrices R_{Z_p}. Hence, even in this situation, the propagation vectors $G_{p,n}$ still constitute the principal eigenvectors of these matrices without noticeable deviations.

Otherwise, for the large capacity scenarios in which we are interested, the noise becomes almost white and uncorrelated, as assumed in this paper, when many users are present in the system. We are presently studying exact solutions in the colored noise case. Such solutions might be useful in particular situations where the distribution is nonuniform in the presence of strong localized interference sources.

Now in the white noise case considered, assuming a perfect power control situation where all the users are received at their corresponding base-stations with a power equal to ψ^2_{opt}, we can write the signal to interference plus noise ratio at the output as follows:

$$SINR_{\text{out}} = \frac{\psi^2_{\text{opt}}}{\sigma^2_{\mathcal{I}}/(2ML)} = \frac{2ML\psi^2_{\text{opt}}}{(C-1)\psi^2_{\text{opt}} + \sigma^2_{\mathcal{O}}} , \qquad (10)$$

where $\sigma^2_{\mathcal{I}}$ is the total received interference power, C is the number of users in the desired cell (*i.e.* capacity), and $\sigma^2_{\mathcal{O}}$ is the power of thermal noise and interference received from the other cells. The interference reduction factor L is due to the processing gain and the beamforming step involves a reduction factor of M, while the Real{.} function in (5) reduces the residual interference by a factor of 2.

The out-of-cell interference is given by $\sigma^2_{\mathcal{O}}=f(C-1)\psi^2_{\text{opt}}$ [1], where f is a factor modeling the total interference contribution in the desired cell of C users in each of the other cells. This factor depends on the propagation parameters, the cell geometry and the type of handoff [1]. In this case the capacity C in terms of users per cell is given by:

$$C = \frac{2ML}{(1+f)(E_b/N_o)} + 1 , \qquad (11)$$

where (E_b/N_o) is the required value of $SINR_{\text{out}}$ for adequate bit error rate performance.

Note here that (E_b/N_o) is the value required before differential decoding of $\hat{b}_n$. After this step, the bit error rate increases by a factor ranging from 1 to 2, depending on the relative location of errors. In the ideal case, where errors are all consecutive in time, the bit error rate remains barely unchanged. In the worst case, where no errors are consecutive, the bit error rate is multiplied by 2 after differential decoding. In the following we provide an analysis of a worst case scenario.

Let us now define the error function by:

$$\text{erf}(x) = \frac{2}{\sqrt{\pi}} \int_0^x e^{-\frac{t^2}{2}} dt . \qquad (12)$$

If the required bit error rate is denoted by p_e, then the required bit energy to noise ratio is given by:

$$\left(\frac{E_b}{N_o}\right) = \left[\text{erf}^{-1}\left(1 - \frac{p_e}{2}\right)\right]^2 . \qquad (13)$$

Using this equation in (11), we can give the capacity as a function of the required bit error rate p_e:

$$C(p_e) = \frac{2ML}{(1+f)\left[\text{erf}^{-1}\left(1-\frac{p_e}{2}\right)\right]^2} + 1 . \qquad (14)$$

If the results of [2] are reformulated following our terminology, then we have:

$$C'(p_e) = \frac{ML}{(1+f)\left[\text{erf}^{-1}(1-p_e)\right]^2} + 1 . \qquad (15)$$

The capacity gain is hence given by:

$$\Delta C(p_e) = \frac{C(p_e)}{C'(p_e)} \simeq \frac{2\left[\text{erf}^{-1}(1-p_e)\right]^2}{\left[\text{erf}^{-1}\left(1-\frac{p_e}{2}\right)\right]^2} . \qquad (16)$$

It is asymptotically independent of the number of sensors M and of the processing gain L.

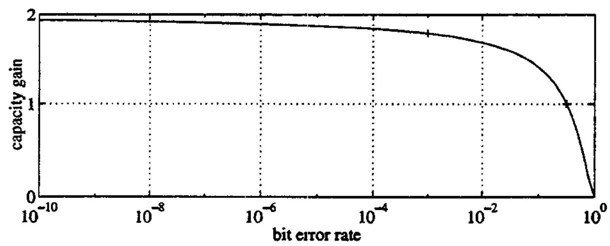

Figure 1: Capacity gain versus the required bit error rate.

In Fig. 1, we plot the curve of the capacity gain of Eq. (16) as a function of the required bit error rate. Note that the capacity gain is higher for lower bit error rates (*e.g.* $\Delta C(p_e) > 1$ for $p_e < 0.32$). It includes the functional values usually required. For instance, for $p_e = 10^{-3}$, the capacity gain is almost of 1.8 in the worst case scenario. The capacity result for STAR is asymptotically greater than that of [2] by almost a factor of 2.

4. SIMULATION RESULTS

We consider for our simulations the case of a code length $L = 64$, a number of sensors $M = 4$ and a number of paths $P = 3$. All the channel parameters vary with time.

In Fig. 2a and 2b, we plot the moduli and angles of propagation vectors $G_{p,n}$ over each sensor and each path. In Fig. 3a, we plot with a dotted line the true received power ψ^2_n without power control. It varies over a dynamic range of 20 dB from -10 dB to 10 dB. To reduce this variation, we fix the required received power to $\psi^2_{\text{opt}} = 1$ (*i.e.* 0 dB). The fraction of total power in each path $\varepsilon^2_{p,n}$ also varies with time as shown in the top sub-plot of Fig. 3b.

We first fix the total interference power $\sigma^2_{\mathcal{I}}$ at 40. In Fig. 4a, we show that Eq. (9) effectively and rapidly tracks

$G_{p,n}$ and reduces average identification error below -35 dB despite all the nonstationarities. With power control, the estimated received power $\hat{\psi}_n^2$, plotted with a solid line in Fig. 3a, is adjusted to ψ_{opt}^2 and its dynamic range is reduced from 20 dB to almost 1 dB. On the other hand, the bottom sub-plot of Fig. 3b shows that the power fractions are properly estimated.

To validate Eq. (10), we now fix the total interference power $\sigma_{\mathcal{I}}^2$ at different values without changing the previous scenario. The experimental values obtained in Fig. 4b fit well with the theoretical curve plotted with a solid line. Should a value of f be fixed, the capacity C in users per cell can be given at any desired bit error rate performance.

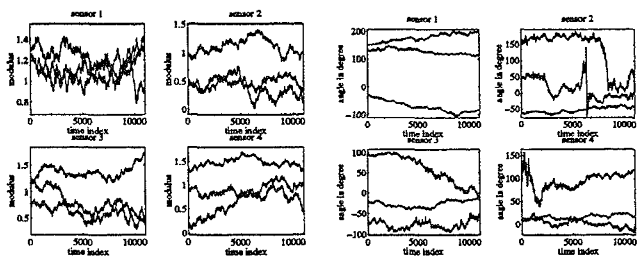

(a) (b)

Figure 2: Propagation vectors for the 3 paths. (a): True moduli. (b): True angles in degree (unwrapped).

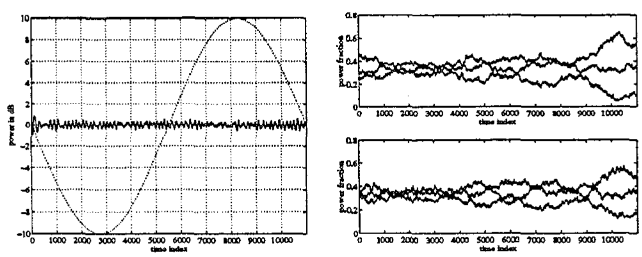

(a) (b)

Figure 3: (a): Received power in dB, true without power control (dotted), estimated with power control (solid). (b): Power partition over the 3 paths, true values (top sub-plot), estimated values (bottom sub-plot).

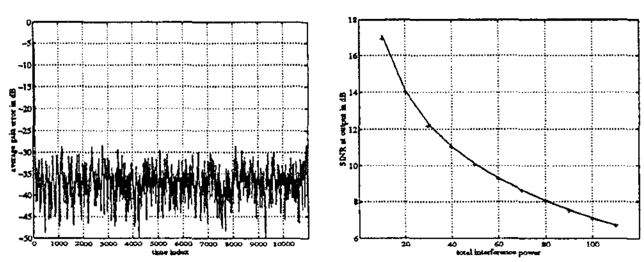

(a) (b)

Figure 4: (a): Average gain error of channel identification $\left(1 \pm \sum_{p=1}^{P} \hat{G}_{p,n}^H G_{p,n}/MP\right)^2$. (b): $SINR_{\text{out}}$ of Eq. (10) versus total interference power $\sigma_{\mathcal{I}}^2 = (1+f)(C-1)$, theoretical (solid), estimated ('+').

5. CONCLUSION

Using a formulation appropriate to array signal processing, we proposed in this contribution a Subspace-Tracking Array-Receiver (STAR) for cellular CDMA which outperforms techniques proposed in [2],[3]:

- STAR is adaptive and shows a fast tracking capability in the presence of strong nonstationarities. It is capable of controlling high variations in received power.

- STAR has a very simple structure and requires an order of computational complexity of $O(MP)$ per bit iteration where M is the number of sensors and P the number of paths.

- STAR asymptotically shows for high bit error rates, theoretically as well as experimentally, a capacity increase in terms of number of users per cell of an order of $O(2M)$, almost twice more than in [2].

At present, we are evaluating the performance of STAR in terms of capacity under realistic conditions, following a thorough methodology presented in [9]. An optimal implementation of STAR in colored noise is also under way.

6. REFERENCES

[1] A.J. Viterbi, *CDMA Principles of Spread Spectrum Communication*, Addison-Wesley, 1995.

[2] B. Suard, A.F. Naguib, G. Xu, and A. Paulraj, "Performance of CDMA mobile communication systems using antenna arrays", *in Proc. ICASSP'93*, vol. IV, 1993, pp. 153-156.

[3] A.F. Naguib and A. Paulraj, "Effects of multipath and base-station antenna arrays on uplink capacity of cellular CDMA", *in Proc. GLOBECOM'94*, 1994, pp. 395-399.

[4] S. Affes and P. Mermelstein, "Spatio-temporal array-receiver for multipath tracking in cellular CDMA", *in Proc. of IEEE ICC'97*, Montréal, Canada, to appear, June 8-12, 1997.

[5] S. Affes, S. Gazor, and Y. Grenier, "An algorithm for multisource beamforming and multitarget tracking", *IEEE Trans. on Signal Processing*, vol. 44, pp. 1512-1522, June 1996.

[6] S. Affes, S. Gazor, and Y. Grenier, "An algorithm for multi-source beamforming and multi-target tracking: further results", *in Proc. EURASIP EUSIPCO'96*, vol. I, 1996, pp. 543-546.

[7] E. Oja, "A simplified neuron model as a principal component analyzer", *J. of Math. Biology*, vol. 15, pp. 267-273, 1982.

[8] B. Yang, "Projection approximation subspace tracking", *IEEE Trans. on Signal Processing*, vol. 43, pp. 95-107, Jan. 1995.

[9] A. Jalali and P. Mermelstein, "Effects of diversity, power control, and bandwidth on the capacity of microcellular CDMA systems", *IEEE J. on Select. Areas in Commun.*, vol. 12, pp. 952-961, June 1994.